

Energy Transfer for Implantable Electronics in the Electromagnetic Midfield

John S. Ho and Ada S. Y. Poon*

(Invited Paper)

Abstract—The wireless transfer of electromagnetic energy into the human body could power medical devices and enable new ways to treat various disorders. To control energy transfer, metal structures are used to generate and manipulate radio-frequency electromagnetic fields. Most systems for transfer across the biological tissue operate in the quasi-static limit, but operation beyond this regime could afford new powering capabilities. This review discusses some recent developments in the design and implementation of systems operating in the electromagnetic midfield, where transfer exploits wave-like fields in the body.

1. INTRODUCTION

Advances in semiconductor technology have opened the possibility of restoring or even augmenting physiological function with electronics. To implant electronic devices into the body, a long-term power source is required. Most current medical devices use batteries, but their bulkiness and limited lifetimes motivate ways to miniaturize them or to substantially increase their lifetimes [1]. One approach is to harvest intrinsic energy sources in the body, such as heat [2], motion [3], glucose [4], or biopotentials [5]. In their existing forms, however, harvesting technologies are anatomically specific and yield low power densities. To overcome these limitations, an electromagnetic source could be used to wirelessly transfer power to implantable devices nearly anywhere in the body.

Energy transfer relies on solutions to Maxwell's equations that carry energy from point to point without wires or waveguides. To direct energy from outside of the body, much research has been devoted to designing suitable electromagnetic structures [6–8]. Most of these structures are typically understood in terms of near-field (quasi-static) approximations to Maxwell's equations. In this approximation, the fields are either primarily electric or magnetic in nature and do not change substantially between air and material. Energy transfer in a nonquasi-static regime could afford additional opportunities and applications, but new designs and tools are required for manipulating fields that propagate and diffract through the body. We review some of our recent work on wireless energy transfer the electromagnetic midfield region, where designs must take into account the wave-like characteristics that emerge from Maxwell's equations.

2. ENERGY TRANSFER INTO THE BODY

2.1. Near-Field Systems

Wireless energy transfer across biological tissue was first demonstrated in the early 1960s, inspired by applications toward an artificial heart [9–11]. High levels of power (ranging from 50 W to 1 kW) were

Received 6 July 2014, Accepted 29 July 2014, Scheduled 7 August 2014

Invited paper for the Commemorative Collection on the 150-Year Anniversary of Maxwell's Equations.

* Corresponding author: Ada S. Y. Poon (adapoon@stanford.edu).

The authors are with the Department of Electrical Engineering, Stanford University, Stanford, California 94305, USA.

targeted over the chest wall thickness, taken to be about 2 to 3 cm. Based on power transformer systems, large planar coils with diameters ranging from 5 to 10 cm were considered for energy transfer through time-varying fields. The fields generated by the coils are primarily magnetic in nature (i.e., quasi-magnetostatic). This regime was considered advantageous because magnetic fields do not interact with biological materials. Interactions due to the nonzero electric field, which result in tissue heating, could be further minimized by operating a relatively low frequency (400 kHz) [11]. From a circuit analysis, it was shown that transfer to the load could be maximized if the receive coil was capacitively tuned to resonate at the operating frequency [9]. The efficiency would then be set by the resonance quality factor and the coupling coefficient between the coils. Energy transfer was demonstrated in animal models [10], although long-term use was impractical due to the large size of the coils, the limited transfer range, and the bulkiness of the external equipment.

Most demonstrations of energy transfer across tissue are based on similar near-field coil configurations [12–18], with major improvements in range and tolerance to geometrical variations. Their design employs a variety of techniques, including quality-factor enhancements [16], adaptive tuning [19], and relay coils [18]. Near-perfect efficiency ($> 70\%$) has been demonstrated across distances comparable to the dimensions of the coils [16–18]. The performance degrades rapidly, but can remain substantial, when the separation is increased to several times the diameter of the coils [20]. Near-field systems are in commercial use in some types of medical electronics, such as cochlear implants, and are anticipated to find wide application in other high-power consumption devices where near-perfect efficiency is critical.

2.2. Miniaturized Electronic Implants

Emerging classes of highly miniaturized, low-power medical electronics are being made possible by advances in integrated circuit (IC) technology and circuit design techniques. These devices employ application-specific designs to achieve power consumption levels and form factors that are orders of magnitude lower than general purpose systems, incorporating sensing, signal processing, data conversion, and communication subsystems into areas on the order of a square millimeter and power consumption levels in the microwatt range [1]. The small size of these devices could enable implantation through catheter delivery or injection through a hypodermic needle, circumventing conventional surgery.

To make such devices practical, they need to be wirelessly powered with structures of compatible sizes — about a millimeter or less in diameter. At this scale, however, near-field coils are highly inefficient for transferring energy to organs such as the heart or brain, which are located many centimeters from the surface. This limitation is a direct consequence of the exponential decay of the evanescent near-field — the range of transfer is limited to distances on the order of the diameter of the smallest coil in the presence of loss [21]. It is argued, however, that such behavior is not intrinsic to electromagnetic transfer and can be overcome in nonquasi-static regimes where propagation and other high-frequency phenomena play a key role [22]. An understanding of these behaviors in context of the body could lead to new, high-performance energy transfer designs.

3. ENERGY TRANSFER THEORY

3.1. Coupled Structures

The analysis of energy transfer starts with a formalism for two coupled systems. In general, such a formalism describes the exchange of energy between specific ports defined at the source and receiver structures. This enables parametrization of the intrinsic losses, the coupling between the structures, and the power extracted by the load through the inputs and outputs at these ports. Various formalisms have been adopted for energy transfer, including impedance parameters [8], scattering matrices [23], and coupled-mode theory [20, 24, 25]. These formalisms differ in the inputs and outputs (specified by voltages, currents, power amplitudes, or modal amplitudes), although all such descriptions are fundamentally based on linearity of Maxwell's equations in the source terms.

From the parameters of the coupling formalism, an expression can be found for the load that maximizes the extracted power. This leads to the classic impedance-matching conditions for energy transfer. It can be shown that transfer is maximized by correctly setting (i) the resonant frequencies of the source ω_S and receiver ω_C and (ii) the rate of energy extraction by the load γ_L . In the weak

coupling regime, it can be shown that the impedance-matching conditions are simply $\omega = \omega_S = \omega_C$ and $\gamma_L = \gamma_C$, where ω is the operating frequency and γ_C the rate of energy loss at the receiver structure [26]. In the strong-coupling regime, the matching conditions differ by a correcting term dependent on the coupling strength due to mode-splitting [19]. For high energy-transfer performance, it is critical for the parameters of the structures and the load to satisfy these conditions.

3.2. Field Specification

The parameters in the coupling formalism are fundamentally defined in terms of the electromagnetic fields. When the receive structure is taken to be a subwavelength coil, it can be shown that the strength of the coupling is determined by the parameter

$$\eta = \frac{\left| \int d^3r B_S^* \cdot M_C \right|^2}{\left[\int d^3r \epsilon'' |E_S|^2 \right] \left[\int d^3r \epsilon'' |E_C|^2 \right]}. \quad (1)$$

where E_S and B_S are the electric and magnetic fields due to the source, E_C the electric field due to the coil, and M_C the magnetization generated by the coil. A time dependency of $e^{-i\omega t}$ has been assumed. In the weak-coupling regime, η can be interpreted as the efficiency of power transfer when the impedance-matching conditions are satisfied.

The source fields can be generated by variety of structures. These structures produce a spatial distribution of currents, which radiate distinct field patterns. Such patterns can be solved from Maxwell's equations by specifying the source current density distribution j_S . For a particular tissue geometry, the solution can be given in terms of the Green's function $G_F(r_\alpha, r_\beta)$ describing propagation between a point on the source r_α and a target point r_β , where the subscript F denotes either the electric (E) or magnetic (B) field. The total radiated field is found from the superposition of the fields radiated by each infinitesimal source element.

3.3. Optimal Energy Transfer Source

The search for a source structure that maximizes energy transfer is important for both practical design and fundamental understanding. The design space, however, is too vast to exhaustively search with full-field electromagnetic simulations. To begin, the field equivalence principle can be invoked to reduce the dimensionality of the search space [26]. The principle is applied by drawing a plane between the surface of the body and the volume outside of the body where sources are allowed to exist. Since every source can be represented by an electric current density in the plane, the search space can be reduced to that of all such current sheets. Each current sheet uniquely specifies a field pattern, since it determines a set of boundary conditions on the body volume.

Further insight into this problem can be obtained by describing energy transfer in the operator formalism. Using Dirac bra-ket notation, we represent the source current sheet by a ket as $j_S \rightarrow |\psi\rangle$ and the coil magnetization as $M_C \rightarrow |\phi\rangle$. The Green's function for the current sheet is represented by the operator G_F ; the full radiated fields are given by $G_F|j_S\rangle$. In this notation, the source-dependent factors (containing the subscript S) in Eq. (1) can be collected and written as

$$f(|\psi\rangle) = \frac{|\langle \phi | G_B |\psi\rangle|^2}{\langle \psi | \epsilon G_E^\dagger G_E | \psi \rangle} \quad (2)$$

where ϵ is a diagonal operator containing the dielectric permittivity at each point. In this notation, it is clear that the numerator in Eq. (2) is an inner product between the source field and the coil magnetization. Furthermore, the denominator can be interpreted as a measure of length, since the operator $\epsilon G_E^\dagger G_E$ is positive-semidefinite (as power loss is necessarily nonnegative). The search for the optimal source can now be posed as an optimization problem maximizing $f(|\psi\rangle)$ over the space of all current sheets. Remarkably, this problem is in the form of the matched-filtering problem [26]. It is straightforward to show from the Cauchy-Schwarz inequality that the solution is $|\psi_{\text{opt}}\rangle = (\epsilon G_E^\dagger G_E)^{-1} G_B |\phi\rangle$ [27].

3.4. Multilayer Model

A starting point for this theory is the multilayer model [Figure 1(a)] for which the Green’s function is analytically known. Computation of the solution can be considerably accelerated in this geometry by representing the source and fields in the angular spectrum (plane-wave basis), which diagonalizes the Green’s function operator [28]. By maximizing Eq. (2) across a wide range of operating frequencies, optimal energy transfer can be established. Figures 1(b)–(e) show the solution for multilayers approximating the chest wall — skin, fat, muscle, bone, and cardiac tissue — at the maximum operating point (1.7 GHz) compared to a coil source. The dielectric properties ϵ of the tissue types are shown in Table 1; the magnetic permeability μ is that of free-space since biological tissue does not exhibit a magnetic response. The receiver is assumed to be a subwavelength coil implanted 5 cm from the sheet, and is impedance-matched at each frequency, subject to constraints on the realizable range of quality factors.

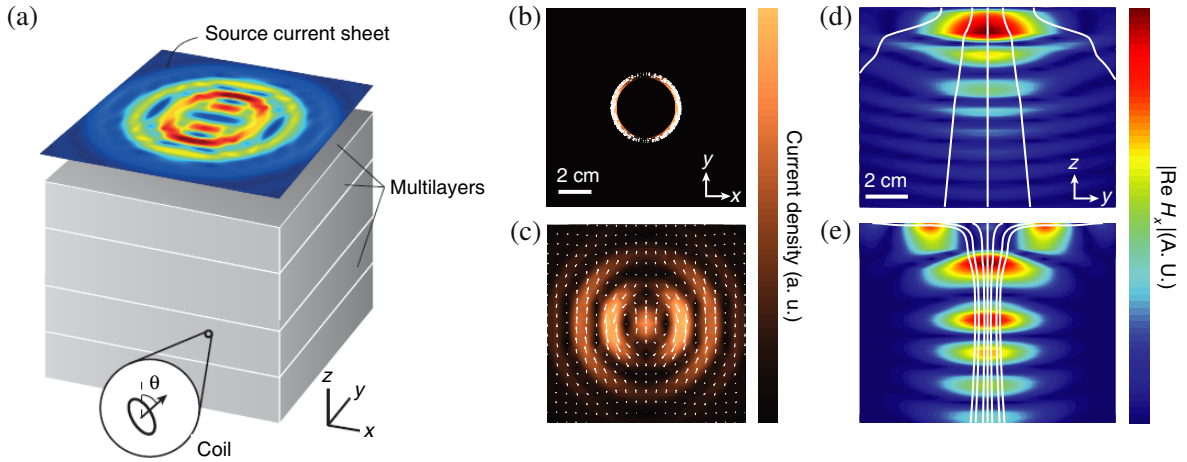


Figure 1. Optimal energy transfer source in a multilayer tissue model. (a) Multilayer model for energy transfer to a subwavelength coil. (b), (c) Source current density for a coil (b) and the optimal solution (c) at the peak-efficiency operating point of 2.6 GHz for a 800- μm diameter coil. The optimal solution is obtained by solving a matched-filtering problem for a coil implanted 5 cm from the current sheet. (d), (e) Magnetic field intensity contour in the multilayers for the coil (d) and optimal current sheet (e). The Poynting flow lines are shown in white.

Table 1. Relative dielectric permittivity of various tissues at 1.6 GHz using Debye dispersion fit [29].

Tissue type	Real part (ϵ'/ϵ_0)	Imaginary part (ϵ''/ϵ_0)
Skin	35.83	5.68
Fat	11.44	1.41
Muscle	53.74	9.3
Bone	20.19	3.66
Heart	53.68	6.45

The resulting current sheet is oscillatory [Figure 1(c)], with peaks spaced less than the wavelength in vacuum, and non-stationary. The currents form surface waves propagating inward towards center point. Figure 1(e) shows that the fields radiated by this current sheet are focused on the device, generating converging Poynting flow lines. The focal spot is much smaller than the wavelength in vacuum. This effect relies on the decrease in wavelength as the wave moves from air into material; full control of the propagating modes supported by the body is key for this method of energy transfer. The characteristics of this “midfield” regime are crucial for high-performance, as the optimal solution in the quasi-static (long-wavelength) limit is about three orders of magnitude less efficient.

3.5. Computational Body Models

For the complex environments such as the human body, application of the theory requires that the Green's function $G(r_\alpha, r_\beta)$ be estimated through numerical simulations. Using a finite subset of points on the source plane, this can be done by positioning an infinitesimal current element at r_α and solving for the radiated fields over all r_β [30]. The resulting matrix can be used to obtain an estimate of the optimal source for the body model. Figure 2(a) shows the efficiency as a function of frequency for the multilayer model and a realistic human body model where the current sheet has been discretized into an array of 550 elements. Around the peak, the efficiency curve is in excellent agreement with the multilayer result. The magnetic field intensity in tissue is shown at the optimal operating point [Figure 2(b)] and at a point in the quasi-static regime [Figure 2(c)]. The distinct features identified from the multilayer model, including non-stationary source currents and focused field patterns, can also be observed in solution for the body model.

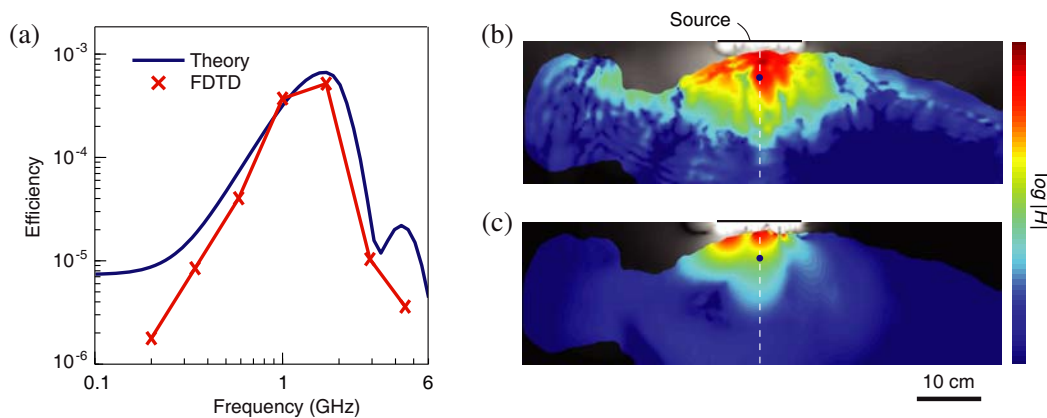


Figure 2. Optimal energy transfer in a computational model of the human body. (a) Transfer efficiency as a function of frequency for a 2-mm diameter coil implanted in the heart. The theory curve is calculated from a multilayer approximation of the chest wall. The finite-difference time-domain (FDTD) curve numerically estimates the optimal current sheet using a discretization of the Green's function. (b) Contour plot of the magnetic field intensity at the peak operating point (1.7 GHz). (c) Contour plot of the magnetic field intensity in the quasi-static regime (200 MHz). The implant position is marked by the blue dot.

4. MIDFIELD ENERGY TRANSFER

To realize midfield energy transfer, the optimal source needs to be implemented by suitable electromagnetic structures. Metal plates provide a myriad of ways to manipulate the pattern of currents on the plate by sizing and shaping various patterns on the plate. A metal plate patterned with circular slots was shown to reproduce the main features of the optimal current sheet [Figure 3(a)]. The structure is excited by four radio-frequency ports [31] with different relative phases, which can be adjusted to control the position of the focal point [Figure 3(b)].

A tiny microelectronic device, containing a coil about 2 mm in diameter, was used to measure power transfer. The device reports the extracted power through the pulsing rate of a light-emitting diode (LED), which can be calibrated precisely for the power transferred to the coil. When transferring energy across a liquid solution mimicking the properties of human tissue, the performance closely approaches that of the theoretical optimum [Figure 3(b)]. The power coupled into the tissue is set to 500 mW, the typical output power of a cell phone. The power transferred to the implant at a distance of 5 cm, for example, is measured to be about 200 μ W. This level is more than sufficient for advanced electronic function; a cardiac pacemaker, in comparison, consumes just 8 μ W [32]. Experiments in porcine tissue in the cardiac [Figure 3(d)] and brain [Figure 3(e)] implant configurations measured 195 μ W and 200 μ W of

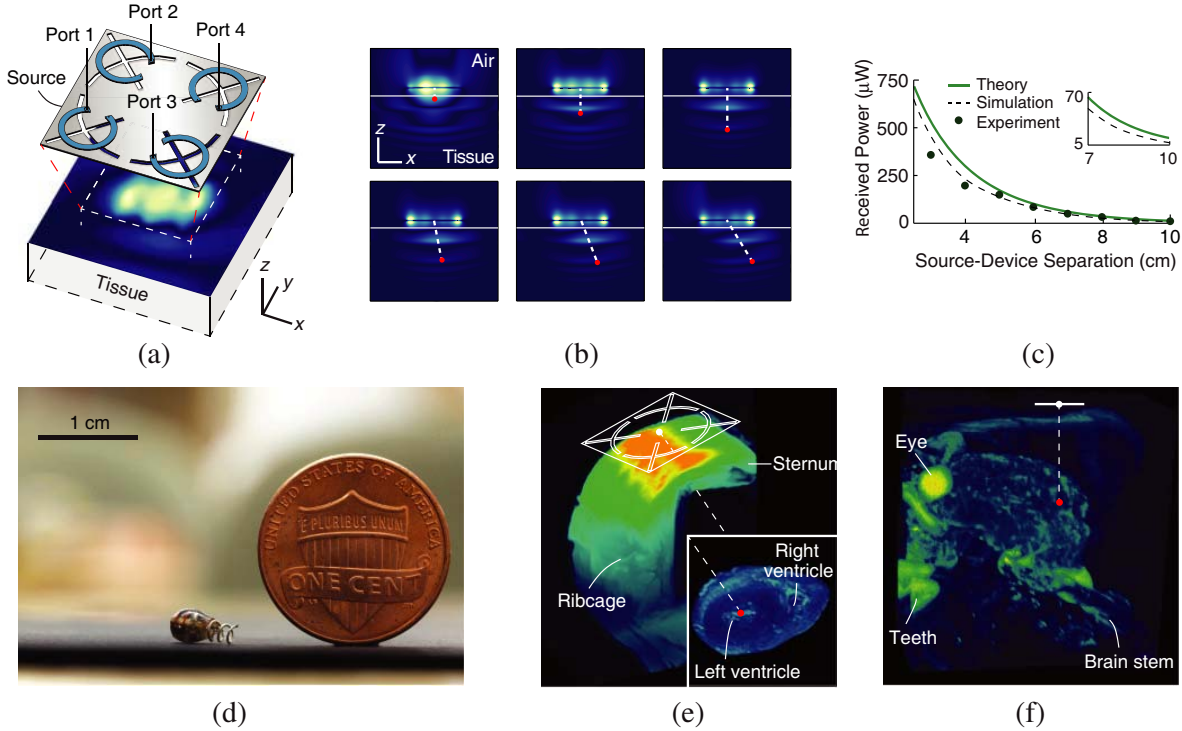


Figure 3. Experimental realization of midfield energy transfer. (a) Patterned metal plate structure for energy transfer. The structure is controlled by the relative phases of the signals at the input ports. (b) Field patterns in tissue with spatially shifted focal points (simulated at 1.6 GHz). (c) Power transfer characteristics in an air-tissue geometry. The harvesting coil on the device is 2 mm in diameter and the power coupled into tissue is 500 mW. Tissue is simulated using a saline solution with measured permittivity $\epsilon/\epsilon_0 = 77.4 + i1.8$. (d) Wireless electrostimulator device. The device is 2 mm in diameter and 3 mm in length (excluding the electrodes) and is powered by the harvesting coil (red) embedded in the device. The silver helical wire is the fixation electrode. (e), (f) Powering configuration in porcine tissue for the heart (e) and brain (f). At an output of 500 mW, the transferred power is measured to be 195 μW and 200 μW respectively. The distance between the source and device (dashed white line) is about 5.5 cm.

transferred power. A microelectronic stimulator, about 2 mm in diameter and 3 mm in length, weighing 70 mg, was powered using this method and used to pace the heart of a rabbit [31]. These results show that energy transfer can be made largely insensitive to fine tissue structure, provided that some phase-adjustment mechanism is available at the source. New design methods based on metasurfaces [33, 34] may afford more precise ways to shape the electromagnetic midfield using similar flat devices.

5. OUTLOOK

This review highlights approaches towards energy transfer into the body that exploit wave-like, rather than quasi-static, fields. The structures used to control these fields are distinct from conventional near-field coils or far-field antennas, which do not account for wave effects predicted by Maxwell's equations. Their design requires new theory aimed at understanding the optimal characteristics of energy transfer and tools exploit these properties. The combination of these approaches with developments in low-power integrated circuits and bioelectronic interfaces is anticipated to lead to new generations of highly miniaturized electronic treatments for disorders in the body.

REFERENCES

1. Chandrakasan, A. P., N. Verma, and D. C. Daly, "Ultralow-power electronics for biomedical applications," *Annu. Rev. of Biomed. Eng.*, Vol. 10, No. 1, 247–274, Aug. 2008.
2. Hochbaum, A. I., R. Chen, R. D. Delgado, W. Liang, E. C. Garnett, M. Najarian, A. Majumdar, and P. Yang, "Enhanced thermoelectric performance of rough silicon nanowires," *Nature*, Vol. 451, No. 7175, 163–167, Jan. 2008.
3. Dagdeviren, C., B. D. Yang, Y. Su, P. L. Tran, P. Joe, E. Anderson, J. Xia, V. Doraiswamy, B. Dehdashti, X. Feng, B. Lu, R. Poston, Z. Khalpey, R. Ghaffari, Y. Huang, M. J. Slepian, and J. A. Rogers, "Conformal piezoelectric energy harvesting and storage from motions of the heart, lung, and diaphragm," *Proc. Natl. Acad. Sci. U.S.A.*, Vol. 111, No. 5, 1927–1932, 2014.
4. Rapoport, B. I., J. T. Kedzierski, and R. Sarpeshkar, "A glucose fuel cell for implantable brain-machine interfaces," *PloS One*, Vol. 7, No. 6, e38436, 2012.
5. Mercier, P. P., A. C. Lysaght, S. Bandyopadhyay, A. P. Chandrakasan, and K. M. Stankovic, "Energy extraction from the biologic battery in the inner ear," *Nat. Biotechnol.*, Vol. 30, No. 12, 1240–1243, 2012.
6. Bashirullah, R., "Wireless implants," *IEEE Microw. Mag.*, Vol. 11, No. 7, 2010.
7. Chow, E. Y., M. M. Morris, and P. P. Irazoqui, "Implantable RF medical devices: The benefits of high-speed communication and much greater communication distances in biomedical applications," *IEEE Microw. Mag.*, Vol. 14, No. 4, 64–73, 2013.
8. Ho, J. S., S. Kim, and A. S. Y. Poon, "Midfield wireless powering for implantable systems," *Proc. IEEE*, 1369–1378, 2013.
9. Schuder, J. C., H. E. Stephenson, Jr., and J. F. Townsend, "High-level electromagnetic energy transfer through a closed chest wall," *IRE Intl. Conv. Rec.*, Vol. 9, 119–126, 1961.
10. Schuder, J. C., H. E. Stephenson, and J. F. Townsend, "Energy transfer into a closed chest by means of stationary coupling coils and a portable high-power oscillator," *ASAIO Trans.*, Vol. 7, 327–331, 1961.
11. Schuder, J. C., "Powering an artificial heart: Birth of the inductively coupled-radio frequency system in 1960," *Artif. Organs*, Vol. 26, No. 11, 909–915, 2002.
12. Flack, F. C., E. D. James, and D. M. Schlapp, "Mutual inductance of air-cored coils: Effect on design of radio-frequency coupled implants," *Med. Biol. Eng.*, Vol. 9, 79–85, 1971.
13. Ko, W. H., S. P. Liang, and C. D. F. Fung, "Design of radio-frequency powered coils for implant instruments," *Med. Biol. Eng. Comput.*, Vol. 15, 634–640, Nov. 1977.
14. Heetderks, W. J., "RF powering of millimeter- and submillimeter-sized neural prosthetic implants," *IEEE Trans. Biomed. Eng.*, Vol. 35, No. 5, 323–327, 1988.
15. Jow, U.-M. and M. Ghovanloo, "Design and optimization of printed spiral coils for efficient transcutaneous inductive power transmission," *IEEE Trans. Biomed. Circuits Syst.*, Vol. 1, No. 3, 193–202, 2007.
16. RamRakhyani, A., S. Mirabbasi, and M. Chiao, "Design and optimization of resonance-based efficient wireless power delivery systems for biomedical implants," *IEEE Trans. Biomed. Circuits Syst.*, Vol. 5, No. 1, 48–63, 2011.
17. Kiani, M., U.-M. Jow, and M. Ghovanloo, "Design and optimization of a 3-coil inductive link for efficient wireless power transmission," *IEEE Trans. Biomed. Circuits Syst.*, Vol. 5, No. 6, 579–591, 2011.
18. Waters, B. H., A. P. Sample, P. Bonde, and J. R. Smith, "Powering a ventricular assist device (VAD) with the free-range resonant electrical energy delivery (free-D) system," *Proc. of the IEEE*, Vol. 100, No. 1, 138–149, 2012.
19. Sample, A. P., B. H. Waters, S. T. Wisdom, and J. R. Smith, "Enabling seamless wireless power delivery in dynamic environments," *Proc. IEEE*, Vol. 101, No. 6, 1343–1358, 2013.
20. Kurs, A., A. Karalis, R. Moffatt, J. D. Joannopoulos, P. Fisher, and M. Soljacic, "Wireless power transfer via strongly coupled magnetic resonances," *Science*, Vol. 317, No. 5834, 83–86, 2007.

21. Lee, J. and S. Nam, "Fundamental aspects of near-field coupling small antennas for wireless power transfer," *IEEE Trans. Antennas Propag.*, Vol. 58, No. 11, 3442–3449, 2010.
22. Poon, A. S. Y., S. O'Driscoll, and T. H. Meng, "Optimal frequency for wireless power transmission over dispersive tissue," *IEEE Trans. Antennas Propag.*, Vol. 58, No. 5, 1739–1749, 2010.
23. Kurokawa, K., "Power waves and the scattering matrix," *IEEE Trans. Microw. Theory Techn.*, Vol. 13, No. 2, 194–202, 1965.
24. Yu, X., S. Sandhu, S. Beiker, R. Sassoon, and S. Fan, "Wireless energy transfer with the presence of metallic planes," *Appl. Phys. Lett.*, Vol. 99, No. 21, 214102, 2011.
25. Kiani, M. and M. Ghovanloo, "The circuit theory behind coupled-mode magnetic resonance-based wireless power transmission," *IEEE Trans. Circuits Syst. I, Reg. Papers*, Vol. 59, No. 8, Aug. 2012.
26. Kim, S., J. S. Ho, and A. S. Y. Poon, "Midfield wireless powering of subwavelength autonomous devices," *Phys. Rev. Lett.*, Vol. 110, No. 20, 203905, May 2013.
27. Poor, V., "Robust matched filters," *IEEE Trans. Inf. Theory*, Vol. 29, No. 5, 677–687, Sep. 1983.
28. Chew, W. C., *Waves and Fields in Inhomogeneous Media*, IEEE Press, Piscataway, NJ, 1995.
29. Gabriel, S., R. W. Lau, and C. Gabriel, "The dielectric properties of biological tissues: III. Parametric models for the dielectric spectrum of tissues," *Phys. Med. Biol.*, No. 41, 2271–2293, Oct. 1996.
30. Kim, S., J. S. Ho, L. Y. Chen, and A. S. Y. Poon, "Wireless power transfer to a cardiac implant," *Appl. Phys. Lett.*, Vol. 101, No. 7, 073701, 2012.
31. Ho, J. S., A. J. Yeh, E. Neofytou, S. Kim, Y. Tanabe, B. Patlolla, R. E. Beygui, and A. S. Y. Poon, "Wireless power transfer to deep-tissue microimplants," *Proc. Natl. Acad. Sci. U.S.A.*, May 2014.
32. Wong, L. S. Y., S. Hossain, A. Ta, J. Edvinsson, D. H. Rivas, and H. Naas, "A very low-power cmos mixed-signal ic for implantable pacemaker applications," *IEEE J. Solid-State Circuits*, Vol. 39, No. 12, 2446–2456, Dec. 2004.
33. Pfeiffer, C. and A. Grbic, "Metamaterial huygens' surfaces: Tailoring wave fronts with reflectionless sheets," *Phys. Rev. Lett.*, Vol. 110, No. 19, 197401, May 2013.
34. Yu, N. and F. Capasso, "Flat optics with designer metasurfaces," *Nat. Mater.*, Vol. 13, No. 2, 139–150, Jan. 2014.